Asymmetric electron energy sharing in strong-field double ionization of helium

Yueming Zhou, Qing Liao, and Peixiang Lu*

Wuhan National Laboratory for Optoelectronics, Huazhong University of Science and Technology, Wuhan 430074, People's Republic of China

(Received 29 July 2010; published 3 November 2010)

With the classical three-dimensional ensemble model, we have investigated the microscopic recollision dynamics in nonsequential double ionization of helium by 800-nm laser pulses at 2.0 PW/cm^2. We demonstrate that the asymmetric energy sharing between the two electrons at recollision plays a decisive role in forming the experimentally observed V-shaped structure in the correlated longitudinal electron momentum spectrum at the high laser intensity [Phys. Rev. Lett. **99**, 263003 (2007)]. This asymmetric energy-sharing recollision leaves footprints on the transverse electron momentum spectra, which provide insight into the attosecond three-body interactions.

DOI: 10.1103/PhysRevA.82.053402 PACS number(s): 32.80.Fb, 32.80.Rm

I. INTRODUCTION

Nonsequential double ionization (NSDI) of atoms in a strong laser field has drawn extensive research in recent years because it provides a particularly clear manner to study the electron-electron correlation, which is responsible for the structure and the evolution of large parts of our macroscopic world [1,2]. The measurements of the recoil ion momentum distributions [3,4], the electron energy distributions [5,6], the correlated two-electron momentum spectra [7,8], as well as numerous theoretical calculations [9–12] have provided convincing evidence that strong-field NSDI occurs in favor of the classical recollision model [13]. According to this model, the first electron that tunnels out of the atom picks up energy from the laser field, is driven back to its parent ion when the field reverses direction, and transfers part of its energy to dislodge a second electron. Though the recollision model describes the NSDI process clearly, the details of recollision remain obscure. For instance, at intensities below the recollision threshold, the underlying dynamics for the intensity-independent $5U_p$ (U_p is the ponderomotive energy) cutoff in the two-electron energy spectra [14–16] and the dominant back-to-back emission of the correlated electrons from NSDI of Ar [15] has not been well explored.

Recently, the high resolution and high statistics experiments on double ionization (DI) of helium have made great progress in unveiling the microscopic recollision dynamics in NSDI. The fingerlike structure in the correlated longitudinal (in the direction parallel to the laser polarization) momentum distribution from NSDI of helium by a 800-nm, 4.5×10^{14} W/cm^2 laser pulse indicates backscattering at the nucleus upon recollision [17]. At a higher intensity, 1.5×10^{15} W/cm^2, Rudenko *et al.* observed a pronounced V-like shape of the correlated two-electron momentum distribution [18], which is interpreted as a consequence of Coulomb repulsion and typical $(e,2e)$ kinematics. Theoretical studies have demonstrated that at the relatively low laser intensity, both the nuclear Coulomb attraction [19,20] and the final-state electron repulsion [20,21] contribute to this structure. However, at the relatively high laser intensity, the roles of final-state electron repulsion and nuclear attraction for the V-like shape have not been examined. It is questionable whether the responsible microscopic dynamics for the V-like shape at this high intensity is similar to that at the relatively low intensity.

In this paper, with the classical three-dimensional (3D) ensemble model [12,22], we examine the microscopic recollision dynamics in NSDI of helium by a high intensity (2.0×10^{15} W/cm^2) laser pulse. We find that the V-like shape of the correlated electron momentum in the direction parallel to the laser polarization is a consequence of the asymmetric electron energy sharing in the recollision process, whereas neither the nuclear attraction nor the final-state electron repulsion contributes to the V-like shape. This is different from that at relatively low intensity, where both the nuclear Coulomb attraction and final-state electron repulsion play significant roles in forming the fingerlike shape. By separating the recolliding electron from the bound electron, we find that the transverse (in the direction perpendicular to the laser polarization) momentum spectra for these two groups of electrons peak at different momenta. This difference is ascribed to the Coulomb focusing in the transverse direction when the electron moves away from the core and can be understood as a footprint of the asymmetric electron energy sharing at recollision.

II. CLASSICAL ENSEMBLE MODEL

The 3D classical ensemble model is introduced in [12] and widely recognized as a useful approach in studying high-field double ionization. In this classical model, the evolution of the two-electron system is governed by Newton's classical equations of motion (atomic units are used throughout this paper unless stated otherwise): $\frac{d^2\mathbf{r}_i}{dt^2} = -\nabla[V_{ne}(r_i) + V_{ee}(r_1,r_2)] - \mathbf{E}(t)$, where the subscript i is the label of the two electrons, and $\mathbf{E}(t)$ is the electric field, which is linearly polarized along the x axis and has a trapezoidal pulse shape with four-cycle turn on, six cycles at full strength, and four-cycle turn off. The potentials are $V_{ne}(r_i) = -2/\sqrt{r_i^2 + a}$ and $V_{ee}(r_1,r_2) = 1/\sqrt{(r_1 - r_2)^2 + b}$, representing the ion-electron and electron-electron interactions, respectively. The soft parameter a is set to 0.75 to avoid autoionization and b is set to 0.01 [12,22,23]. To obtain the initial value, the ensemble is populated starting from a classically allowed position for the helium ground-state energy of -2.9035 a.u. The available kinetic energy is distributed between the two electrons randomly in momentum space, and then the electrons

*Corresponding author: lupeixiang@mail.hust.edu.cn

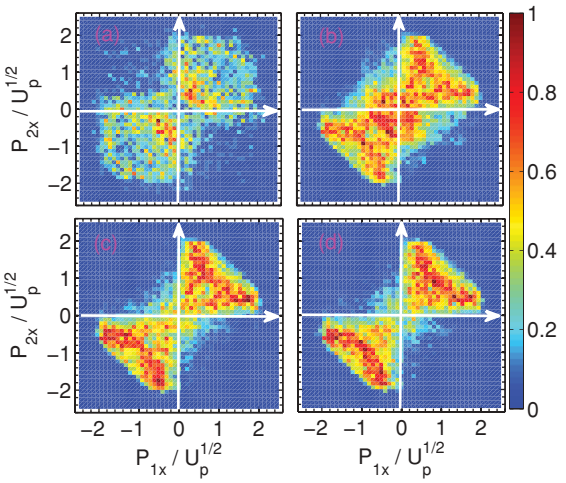

FIG. 1. (Color online) Correlated longitudinal electron momentum distributions for NSDI of helium by 800-nm laser pulses. The intensities are (a) 0.5 PW/cm^2 and (b)–(d) 2.0 PW/cm^2. In (c) and (d), the trajectories where DI occurs at the turn-on stage of the trapezoidal pulse are excluded. In (d), the final-state e-e repulsion is neglected by replacing the soft Coulomb repulsion with the Yukawa potential (see the text for details). The ensemble sizes are 2×10^6.

are allowed to evolve a sufficiently long time in the absence of the laser field to obtain stable position and momentum distributions [16]. Note that in the classical model the first electrons are ionized above the suppressed barrier and no tunneling ionization occurs.

III. RESULTS AND DISCUSSIONS

Figures 1(a) and 1(b) display the correlated electron momentum distributions in the direction parallel to the laser polarization, where the laser intensities are 5.0×10^{14} W/cm^2 and 2.0×10^{15} W/cm^2, respectively. At 5.0×10^{14} W/cm^2, the experimental observed fingerlike structure is not reproduced [Fig. 1(a)]. This is because of the large soft parameter employed in our calculation, which shields the nuclear potential seriously. Previous studies have illustrated that the fingerlike structure is able to be reproduced when the realistic Coulomb potential or a softened potential with a smaller screening parameter is used [19,20].

At the relatively high intensity, the overall V-like shape in the correlated momentum distribution is obvious. In contrast to the previous experimental result [18], a cluster of distribution around zero momentum is clearly seen. Back analysis reveals that these events correspond to the trajectories where DIs occur at the turn-on stage of the laser pulse. For the soft potential employed in this paper, the potential-energy well for the second electron is $-2/\sqrt{0.75} \simeq -2.3$ a.u., which is lower than that of realistic helium. In the classical description, the first electron can get ionized more easily at the expense of leaving the second electron near the bottom of the potential well [24]. Thus the first electron can be ionized very early at the turn-on stage of the pulse, leading to recollision that occurs at the turn-on stage. This effect results in an overestimated contribution from the turn-on stage of the laser pulse to DI. In order to overcome this deficiency and focus our study on the high intensity regime, we artificially exclude the events in which DI occurs at the turn-on stage of the laser pulse, as shown in Fig. 1(c). The correlated electron momentum distribution agrees excellently well with the experiment [18] and the V-like shape is obvious though a soft parameter as large as $a = 0.75$ is employed. We also performed further calculations by changing the soft parameter a after the first ionization [16,19], and no noticeable change has been found in the V-like shape. It implies that the nuclear attraction does not contribute to the V-like shape, which is different from that at the relatively low laser intensity [19,20].

It has been confirmed that at the relatively low intensity, the final-state electron repulsion plays an important role for the fingerlike shape of the correlated electron momentum distribution [20,21]. In order to examine the role of final-state electron repulsion in forming the V-shape at the high intensity, we have performed an additional calculation, in which the final-state electron interaction $V_{ee}(r_1,r_2) = 1/\sqrt{(r_1 - r_2)^2 + b}$ is replaced by $V_{ee}(r_1,r_2) = \exp[-\lambda r_b]/r_b$, where $r_b = \sqrt{(r_1 - r_2)^2 + b}$ and $\lambda = 5.0$ [20]. As shown in Fig. 1(d), the V-like shape is still clearly seen, and no noticeable difference is found when compared to Fig. 1(c). Thus it confirms that the V-like shape is not a consequence of the final-state electron repulsion at this high intensity.

The preceding analysis illustrates that neither the nuclear attraction nor the final-state electron repulsion contributes to the V-like shape in the correlated longitudinal electron momentum at the high laser intensity. In order to explore the responsible dynamics for the V-like shape, we take further advantage of back analysis [11]. Tracing the classical DI trajectories allows us to easily determine the recollision time and the energy exchange during recollision. Here, the recollision time is defined to be the instant of the closest approach after the first departure of one electron from the core [12].

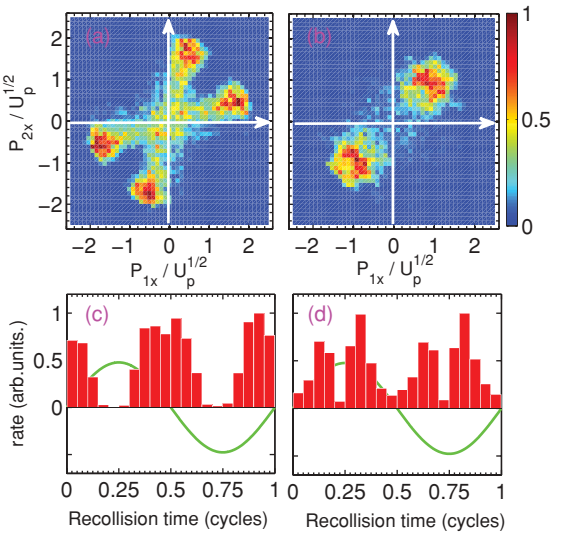

FIG. 2. (Color online) Correlated longitudinal electron momentum distributions for the trajectories where the energy difference at time $0.02T$ after recollision is (a) larger than 2 a.u. and (b) smaller than 2 a.u. (c) and (d) DI yield versus laser phase at recollision for the events in (a) and (b), respectively. The solid green curves represent laser fields. In all plots, the events where DI occurs at the turn-on stage of the trapezoidal pulse are excluded.

In Figs. 2(a) and 2(b), we have segregated the trajectories shown in Fig. 1(c) according to the energy difference of the two electrons at time $0.02T$ after recollision. (T is the laser period. We have changed the time from $0.02T$ to $0.05T$ and the conclusions below do not change with the variation of this time.) Figures 2(a) and 2(b) display the correlated longitudinal electron momentum distributions of the trajectories where the energy difference is larger and less than 2.0 a.u., respectively. It is clearly shown that the events are clustered on the main diagonal when the two electrons achieve similar energies at recollision [Fig. 2(b)]. In contrast, the correlated electron momentum distribution exhibits distinct off-diagonal features when asymmetric energy sharing (AES) occurs [Fig. 2(a)]. Based on these results, we can conclude that the AES at recollision is the decisive reason for the V-like shape in the longitudinal electron momentum correlation at the high laser intensity.

In order to further understand the AES at this high laser intensity, in Figs. 2(c) and 2(d) we present the counts of DI trajectories versus laser phase at recollision. Figures 2(c) and 2(d) correspond to the trajectories from Figs. 2(a) and 2(b), respectively. It is found that in Fig. 2(c), where AES occurs, recollisions cluster around the zero crossing of the laser field, while in Fig. 2(d), recollisions occur close to the extremum of the field. According to the simple-man model [13], the electrons with the maximal recolliding energy return to the core near the zero crossing of the laser field, while those returning to the core near the extremum of the field possess lower recolliding energies. Figures 2(c) and 2(d) imply that the energetic recollisions often favor AES while the less energetic ones tend to have more symmetric energy sharing (SES). After distinguishing the recolliding electrons from the bound electrons we find that for 88% of the AES events [the events in Fig. 2(a)] the energy of the recolliding electron just after recollision is higher than that of the bound electron. It indicates that in the high returning-energy recollision, the recolliding electron only transfers a small part of its energy to the bound electron. This issue is consistent with a recent study [25] in which it was demonstrated that the efficacy of electron-electron collisions decreases with an increase of collision energy. This behavior is easy to understand. For the high returning-energy recollision, the recolliding electron passes the core very quickly, thus the time of the *e-e* interaction is so short that the recolliding electron can transfer only a small part of its energy to the bound electron, resulting in the serious AES at the high laser intensity. One issue should be mentioned that due to the spreading of the electron wave packet, the returning electron often collides with the ion with a sizable impact parameter and the impact parameter of the returning electron can influence the energy exchange during recollision. At the relatively low laser intensity, the Coulomb focusing can significantly decrease the impact parameter when the returning electron passes the efficient area of the ion [26], resulting in a considerable amount of hard recollisions [20]. While at the high intensity, the returning electron passes the efficient area of the ion so fast that the Coulomb focusing effect is weak [27]. Thus the impact parameter is hardly decreased. As a result, the hard recollision is seldom at the high laser intensity.

At the relatively low laser intensity, because of the lower recolliding energy, the recolliding electron passes the core

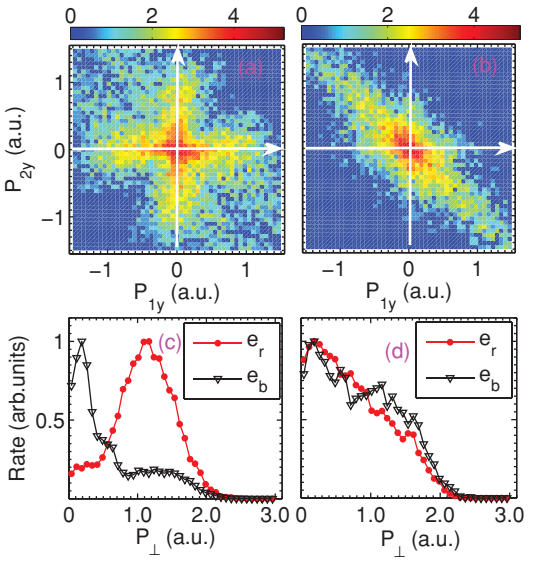

FIG. 3. (Color online) (a) and (b) Joint-probability distributions (on a logarithmic scale) of the transverse momenta (along the y axis) for the trajectories from Figs. 2(a) and 2(b), respectively. (c) Transverse momentum spectra of recolliding (red cycle) and bound (black triangle) electrons for the trajectories from (a). (d) The same as (c) but for the trajectories from (b).

with a small velocity, and thus the time of the *e-e* interaction (i.e., recolliding) is long enough for the recolliding electron to transfer a considerable part of its energy to the bound electron through *e-e* interaction. Consequently, AES is not serious and its contribution to the fingerlike structure is negligible. At the high laser intensity, the short *e-e* interaction time leads to the low-energy exchange efficacy at recollision, which makes AES play the dominant role in forming the V-like shape in the correlated electron momentum spectrum. Because of the dramatic AES, the two electrons leave the core with very different initial momenta and separate quickly. As a consequence, the final-state electron repulsion is weak and does not contribute to the V-like shape.

More details of recollision can be obtained by inspecting the transverse momenta because the subtleties of the momentum exchange in the recollision process are not covered by the much larger momentum transfer taken from the laser field [28]. In Figs. 3(a) and 3(b) we present the joint-probability distributions of the transverse momenta (along the y axis) for the events shown in Figs. 2(a) and 2(b), respectively. Remarkably, in Fig. 3(b) the distribution lies along the diagonal $p_{1y} + p_{2y} = 0$. This behavior indicates the strong repulsion in the transverse direction, which is in agreement with previous studies [28]. Contrarily, in Fig. 3(a) the population is clustered along the axes $p_{1y} = 0$ and $p_{2y} = 0$, indicating different amplitudes of transverse momenta of the two electrons. This difference is clearer when separating the bound electrons from the recolliding ones. In the bottom of Fig. 3 we display the transverse momentum ($P_{i\perp} = \sqrt{p_{iy}^2 + p_{iz}^2}$) spectra of the recolliding (red circle) and the bound (black triangle) electrons separately, where Figs. 3(c) and 3(d) correspond to the events from Figs. 3(a) and 3(b), respectively. For the SES trajectories

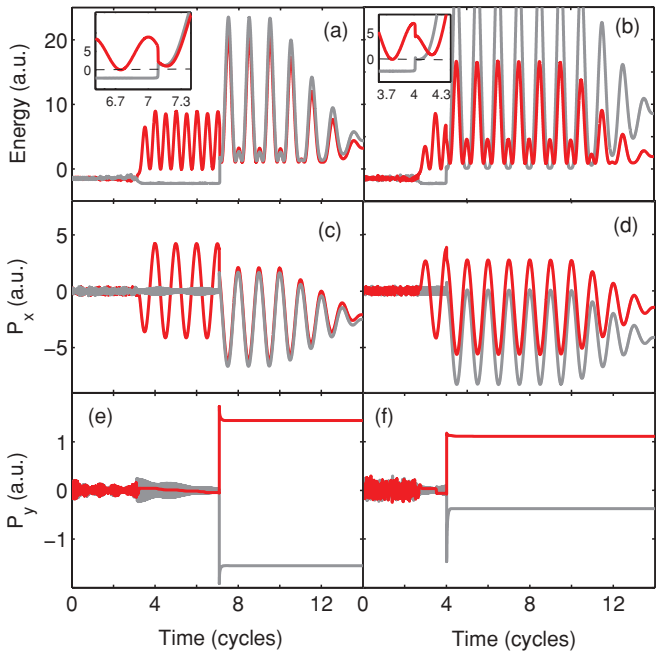

FIG. 4. (Color online) Two sample trajectories selected from Fig. 2(a) (right column) and Fig. 2(b) (left column), respectively. The upper, middle, and bottom rows show the energy, longitudinal momentum, and transverse momentum (along the y axis) versus the time for each electron, respectively. The energy exchange at recollision is clearly visible in the insets of (a) and (b).

[Fig. 3(d)], the recolliding and the bound electrons exhibit similar transverse momentum distributions, whereas for the AES ones [Fig. 3(c)], the difference in the distributions of the recolliding and bound electrons is remarkable: the spectrum of the bound electrons peaks near 0.2 a.u., while for the recolliding electrons the spectrum exhibits a maximum at 1.2 a.u. The different transverse momentum distributions for the SES and AES trajectories imply the different three-body interactions, which can be explored by monitoring the history of the DI events.

We display two sample trajectories in Fig. 4. In the left column, the two electrons have equal energy after recollision [Fig. 4(a)], and achieve similar final longitudinal momentum [Fig. 4(c)]. For the trajectory shown in the right column, the two electrons share unequal energies upon recollision. The recolliding electron (solid red curve) obtains a higher energy at recollision [Fig. 4(b)] but achieves a smaller final longitudinal momentum [Fig. 4(d)] due to the postcollision velocity [12]. The time evolution of the transverse momentum is more interesting. As shown in the bottom of Fig. 4, for both trajectories the two electrons obtain similar transverse momenta with opposite directions upon recollision. For the SES trajectories, both electrons experience a small sudden decrease in the transverse momenta just after recollision [Fig. 4(e)]. For the AES trajectory, the bound electron suffers a much larger sudden decrease in the transverse momentum while the transverse momentum of the recolliding electron does not change after recollision [Fig. 4(f)]. We ascribe the sudden decrease of the transverse momentum to the nuclear attraction in the transverse direction when the electron moves away from the core. For the SES trajectories, the two electrons leave the core with similar momentum, thus the nuclear attraction plays a similar role in decreasing the transverse momentum, resulting in the distribution along the diagonal $p_{1y} + p_{2y} = 0$ in Fig. 3(b). For the AES trajectory, the nucleus does not effect the transverse momentum of the recolliding electron because it leaves the core with a very fast initial momentum. While for the bound electron, it takes a longer time to leave the effective area of the core due to the small initial momentum, leading to a significant decrease of the transverse momentum caused by nuclear attraction. The transverse momentum change of the electron is determined by $\Delta p_\perp = \int F_\perp dt$, where $F_\perp$ is the transverse force of the nuclear attraction. Assuming an electron that starts at a field zero near the region $x = 2$ a.u. with an initial momentum $v_\perp = 1.2$ a.u. and evolves in the combined laser and Coulombic field, it takes a time of about 10 a.u. for the nucleus to decrease $v_\perp$ to 0.2 a.u.

Simply speaking, after recollision, the two electrons leave the core with different initial momenta because of the asymmetric energy sharing during recollision. As a consequence, the nuclear attraction plays different roles in "focusing" the transverse momenta of the bound and recolliding electrons when they move away from the core, resulting in the momentum distributions in Fig. 3(c). In other words, the different transverse momentum distributions of the recolliding and bound electrons reflect the AES at recollision and provide insight into the attosecond three-body interactions.

IV. SUMMARY

In conclusion, we have investigated the attosecond recollision dynamics in NSDI of helium at 2.0×10^{15} W/cm^2. At the high intensity, the bound electron often shares a small part of the recolliding energy at recollision due to the low efficacy of energy exchange at the high recolliding energy. This asymmetric energy sharing is the decisive reason for the observed V-like shape in the correlated longitudinal momentum spectrum at the high laser intensity. Because of the asymmetric energy-sharing recollision, the bound electron leaves the core with a small initial momentum. Thus its transverse momentum is strongly focused by the nuclear attraction when it moves away from the core, whereas the recolliding electron leaves the core so fast that its transverse momentum is not effected by the nuclear attraction. The different transverse momentum spectra of the recolliding and bound electrons act as a signature of the asymmetric energy sharing at recollision and provide insight into the attosecond three-body dynamics.

ACKNOWLEDGMENTS

This work was supported by the National Natural Science Foundation of China under Grant No. 10774054, National Science Fund for Distinguished Young Scholars under Grant No. 60925021, and the 973 Program of China under Grant No. 2011CB808103.

[1] Th. Weber *et al.*, Nature (London) **405**, 658 (2000).
[2] A. Becker, R. Dörner, and R. Moshammer, J. Phys. B **38**, S753 (2005).
[3] R. Moshammer *et al.*, Phys. Rev. Lett. **84**, 447 (2000).
[4] A. Rudenko, K. Zrost, B. Feuerstein, V. L. B. deJesus, C. D. Schroter, R. Moshammer, and J. Ullrich, Phys. Rev. Lett. **93**, 253001 (2004).
[5] R. Lafon, J. L. Chaloupka, B. Sheehy, P. M. Paul, P. Agostini, K. C. Kulander, and L. F. DiMauro, Phys. Rev. Lett. **86**, 2762 (2001).
[6] J. L. Chaloupka, J. Rudati, R. Lafon, P. Agostini, K. C. Kulander, and L. F. DiMauro, Phys. Rev. Lett. **90**, 033002 (2003).
[7] B. Feuerstein *et al.*, Phys. Rev. Lett. **87**, 043003 (2001).
[8] R. Moshammer *et al.*, J. Phys. B **36**, L113 (2003).
[9] M. Lein, E. K. U. Gross, and V. Engel, Phys. Rev. Lett. **85**, 4707 (2000).
[10] A. Becker and F. H. M. Faisal, J. Phys. B **38**, R1 (2005).
[11] Phay J. Ho, R. Panfili, S. L. Haan, and J. H. Eberly, Phys. Rev. Lett. **94**, 093002 (2005).
[12] S. L. Haan, L. Breen, A. Karim, and J. H. Eberly, Phys. Rev. Lett. **97**, 103008 (2006).
[13] P. B. Corkum, Phys. Rev. Lett. **71**, 1994 (1993).
[14] J. S. Parker, B. J. S. Doherty, K. T. Taylor, K. D. Schultz, C. I. Blaga, L. F. DiMauro, and A. Rudenko, Phys. Rev. Lett. **96**, 133001 (2006).
[15] Y. Liu, S. Tschuch, A. Rudenko, M. Durr, M. Siegel, U. Morgner, R. Moshammer, and J. Ullrich, Phys. Rev. Lett. **101**, 053001 (2008).
[16] Y. Zhou, Q. Liao, and P. Lu, Phys. Rev. A **80**, 023412 (2009).
[17] A. Staudte *et al.*, Phys. Rev. Lett. **99**, 263002 (2007).
[18] A. Rudenko, V. L. B. deJesus, T. Ergler, K. Zrost, B. Feuerstein, C. D. Schroter, R. Moshammer, and J. Ullrich, Phys. Rev. Lett. **99**, 263003 (2007).
[19] S. L. Haan, J. S. Van Dyke, and Z. S. Smith, Phys. Rev. Lett. **101**, 113001 (2008).
[20] D. F. Ye, X. Liu, and J. Liu, Phys. Rev. Lett. **101**, 233003 (2008).
[21] Z. Chen, Y. Liang, and C. D. Lin, Phys. Rev. Lett. **104**, 253201 (2010).
[22] Y. Zhou *et al.*, Opt. Express **18**, 632 (2010).
[23] Y. Zhou, Q. Liao, and P. Lu, Opt. Express **18**, 16025 (2010).
[24] S. L. Haan *et al.*, J. Phys. B **42**, 134009 (2009).
[25] F. Mauger, C. Chandre, and T. Uzer, Phys. Rev. Lett. **104**, 043005 (2010).
[26] Thomas Brabec, Misha Yu. Ivanov, and Paul B. Corkum, Phys. Rev. A **54**, R2551 (1996).
[27] C. Huang *et al.*, Opt. Express **18**, 14293 (2010).
[28] M. Weckenbrock, A. Becker, A. Staudte, S. Kammer, M. Smolarski, V. R. Smolarski, D. M. Rayner, D M. Villeneuve, P. B. Corkum, and R. Dorner, Phys. Rev. Lett. **91**, 123004 (2003); **92**, 213002 (2004).